

A HELICAL INVERTED-F ANTENNA MONTED ON GROUNDPLANE EDGE

Nobuhiro KUGA⁽¹⁾, Kenji OBINATA⁽¹⁾, Hidenao MATSUSHIMA⁽²⁾, Naohisa GOTO⁽³⁾

⁽¹⁾*Faculty of Engineering, Tokyo Institute of Polytechnics, 1583 Iiyama, Atsugi-shi, Kanagawa, 243-0297 JAPAN*

E-mail: kuga@ee.t-kougei.ac.jp

⁽²⁾*Mitsubishi Materials Corporation, 2270 Yokoze, Chichibu, Saitama 368-8502, JAPAN*

⁽³⁾*Faculty of Engineering, Takushoku University, 815-1 Yakata-cho, Hachioji-shi, 193-0825, JAPAN*

ABSTRACT

This paper presents an inverted-F antenna miniaturized by helix element printed on a dielectric chip. Its characteristics are examined by using the FDTD calculation and verified by experiments. The results show that the beginning turn of helix-element affects input impedance of inverted-F antenna, and that helix turns in radiating portion affects the resonance frequency. As a result, resonant frequency of the 3-turn HIFA with $\epsilon_r=10.2$ is about 50% lower than that of no-helix inverted-F antenna on the groundplane-edge. It is also confirmed that the helical element configuration has little influence on its radiation pattern.

INTRODUCTION

The short-distance wireless data communication systems such as the Bluetooth requires small and surface-mountable built-in antenna. Planer inverted-F antennas (PIFA) are well known as built-in antenna for portable handsets, however it is too large compared with chip devices such as L, C and R. Concerning the installation of antenna inside a card-shaped terminal, for example, the antenna must be surface-mountable, and be miniaturized to the dimension of the other chip devices [1][2][3]. On the other hand, a demand for the chip antenna that can be operated at the groundplane-edge is also increasing to realize stable radiation gain. However, good matching state is not obtained for the conventional PIFA at the groundplane-edge because its radiation resistance is small such as 17Ω . This paper presents a small inverted-F antenna suitable for edge-mount on a circuit substrate. It is shown that the square helix and a dielectric chip miniaturize the antenna, and validity of the miniaturized inverted-F antenna is verified by using FDTD method and experiments.

FEEDING STRUCTURE OF HIFA MOUNTED AT GROUNDPLANE-EDGE

At first, matching technique of a helical inverted-F antenna (HIFA) mounted on a groundplane edge is discussed. Fig.1 shows an analysis model, where a rectangular disk of $W_e \times L_e$ [mm] is placed parallel beside a groundplane with the separation of d [mm]. Lengths of Feeding and shorting strips are L_f and L_s , respectively. The FDTD analysis with 8-layer PML is applied to the analysis region of $60 \times 60 \times 20$ [mm] using the Yee-cells of $0.5 \times 0.5 \times 0.5$ [mm].

Fig.2 shows calculated input impedances as a function of feeding stripline length L_f when $L_s = W_e + d$. It indicates that the length of feeding probe may control only the reactance while the radiation resistance keeps almost 50Ω . By using this feeding structure, good matching condition is obtained at 2GHz band as shown in fig.3. Therefore, it is shown that the beginning turn of shorting helix contributes to increase of radiation resistance, and the length of the feeding strip affects the input reactance of HIFA. Incidentally, only the poor matching state is achieved when $L_f = L_s = d$, because the radiation resistance is less than 17Ω . A combination of long feeding strip and shorting strip such as $L_f = L_s = W_e + d$ also cause poor matching to the 50Ω because of large inductive reactance.

CHARACTERISTICS OF HIFA

In this section, the effects of helical element with dielectric chip are evaluated by using the FDTD method. Fig.4 shows a configuration of the HIFA with 3-turn helix element. The helical strip is printed on a dielectric chip of $24 \times 14 \times t$ [mm] and relative permittivity of ϵ_r . The number of helix turn is defined as N in this paper.

Before examining the resonance characteristics of the HIFA, effect of groundplane size is examined experimentally. Fig.5 shows the measured resonant frequency for each groundplane dimension, in which (a) and (b) show the dependency on the groundplane width W_g and the length L_g , respectively. In the figure (a), the antenna with $N=0$ and

the dielectric chip of $\epsilon_r=2.6$ is chosen. F_L and F_H are lower and upper limit frequencies in the return loss -10dB bandwidth, and F_c is the center frequency in the bandwidth. F_{\min} shown as a reference in the figures is the frequency with the smallest reflection, which is almost equal to F_c for $W_g < 120$. It is shown that the dependency of F_c on W_g is less than 13% concerning the groundplane width $W_g < 120$. On the other hand, the figure (b) shows the resonant frequency for each groundplane length L_g , where the groundplane width W_g is 80mm. It indicates that the dependence of the resonant frequency is smaller than that of groundplane width, and may be negligible in this case. Therefore the influence of the groundplane dimension may be estimated less than 13% due to the groundplane width W_g .

We use two different analysis conditions for the FDTD analysis to save computing time. One is for the dielectric chips of $\epsilon_r=1$ and 2.6, that includes the analysis region of $80 \times 104 \times 16$ [mm] divided by the Yee cell of $0.4 \times 0.4 \times 0.4$ [mm]. The other is for $\epsilon_r=10.2$ and 4.7, in which the sub-grid with $\Delta x = \Delta y = 0.4$ [mm] and $\Delta z = 0.1$ [mm] is employed inside the dielectric chip region. Time responses are calculated over 7.2nS for $\epsilon_r=4.8$ and 10.2, and 3.2nS for $\epsilon_r=2.6$ and 1.0. Fig.6 shows calculated results of $\epsilon_r=2.6$ and 10.2, in which measurements are also plotted as broken lines. Although the error of bandwidth is conspicuous, the validity of analysis is confirmed with the viewpoint of resonant frequency evaluation.

Fig.7 shows the resonant frequency (F_c) characteristics as functions of the helix turn N and the relative permittivity of the dielectric chip. By increasing N from 0 to 3 in the figure, the resonance frequencies decrease 44, 45, 53% for $\epsilon_r=1, 2.6, 4.8$, respectively. Though the helix element miniaturizes the HIFA, dependence on the dielectric constant is only 10%. It indicates that the miniaturization of the PIFA depends on the helix form of the element much more than the dielectric constant of the core chip. On the other hand, when the material of $\epsilon_r=10.2$ is used, the resonant frequencies decrease 17.5, 18.2, and 17.7% for the helix turn $N=1, 2, 3$, respectively. Incidentally, when $\epsilon_r=10.2$ and $N=3$ are chosen, the resonant frequencies of HIFA are made 54% lower than those of PIFA at the groundplane-edge (Fig.1).

The effective permittivity ϵ_{re} of the dielectric chip material may be evaluated here by using following equation:

$$\epsilon_{re} = \left(\frac{f_1}{f_{\epsilon r}} \right)^2 \quad (1)$$

where the resonant frequency of the HIFA with $\epsilon_r=1$ is f_1 , the one of the antenna with ϵ_r is $f_{\epsilon r}$. Table 1 summarize the results for $\epsilon_r=2.6, 4.8, 10.2$. Though there is some dispersion, the effective permittivity is not affected by the helix turn N . The actual effective permittivity of the HIFA decreases extremely the characteristic permittivity of the material, the dielectric chip of $\epsilon_r=2.6 \sim 10.2$ works as one with $\epsilon_{re}=1.1 \sim 1.5$. Incidentally, change in resonance frequency cannot be ignored though an effective permittivity is low when bandwidth of the antenna is narrow. Effects of helical strip width are also evaluated. Resonant frequency is quite critical to the strip-width in radiating portion, however, strip-width in feeding loop portion does not have large effect on the resonant frequency. The beginning turn of HIFA has an effect only on matching condition.

Finally, influence of miniaturization by the helix element to the radiation pattern is examined. Fig.8 is the amplitude characteristic of the radiation power, in which the solid lines show the HIFA with $\epsilon_r=1, N=0$, and the broken lines show the HIFA with $\epsilon_r=2.6, N=3$. Element thickness $t=1.6$ [mm] is chosen for the both antennas. Though remarkable change is observed only in the yz -plane, the miniaturization by helix element does not affect the radiation pattern very much.

CONCLUSION

The helical inverted-F antenna mounted at a groundplane edge was proposed in this paper. Its basic characteristics were analyzed by the FDTD method and verified by experiments. The results showed that the beginning turn of the helix element affected matching condition to the 50Ω systems, and that helix turns in radiating portion affected the resonance frequency. As a result, resonant frequency of the 3-turn HIFA with $\epsilon_r=10.2$ was about 50% reduced for no-helix inverted-F antenna at the groundplane edge. It was also confirmed that the helical element configuration had little affect on its radiation pattern.

REFERENCES

- [1] N.Goto, "Printed Qubic Antennas," Proceeding of the 1997 IEICE general conference, B-1-70, March 1997
- [2] H.Arai, Y.Tanaka, N.Goto, "FDTD Analysis of Printed Loop Antenna on Dielectric Cube," Proceeding of the 1997 IEICE general conference, B-1-123, March 1997
- [3] D.Yamamoto, H.Arai, "FDTD Analysis of Dielectric Chip Antenna," Proceeding of the 1999 IEICE general conference, B-1-115, March 1999

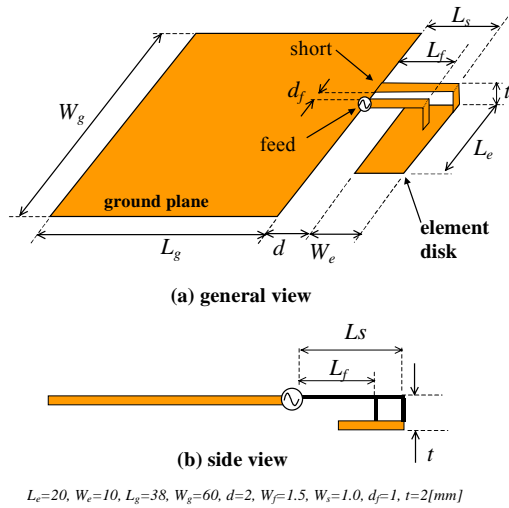


Fig.1. Analysis model for feeding structure of HIFA on the groundplane-Edge

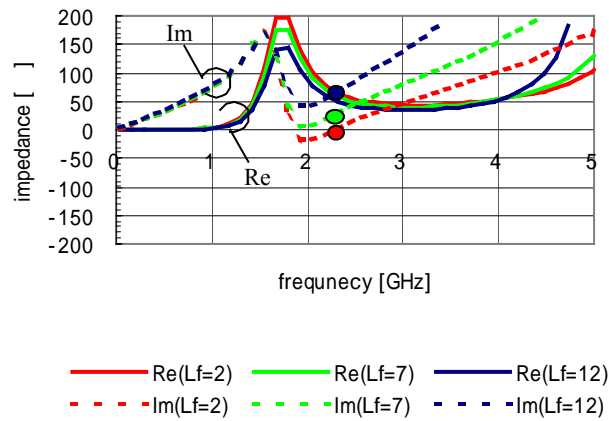


Fig.2. Input impedance characteristics as a function of feeding line length

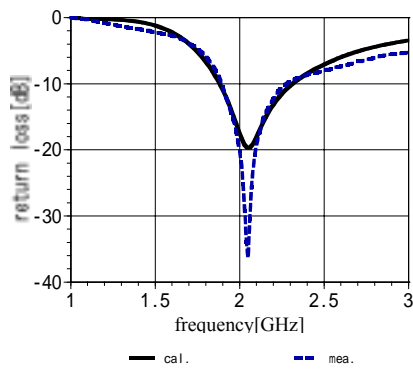


Fig.3. Input characteristics of HIFA (N=0)

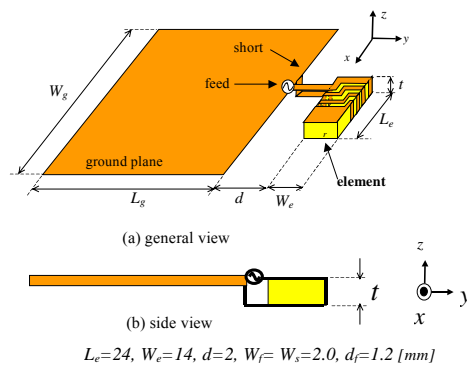
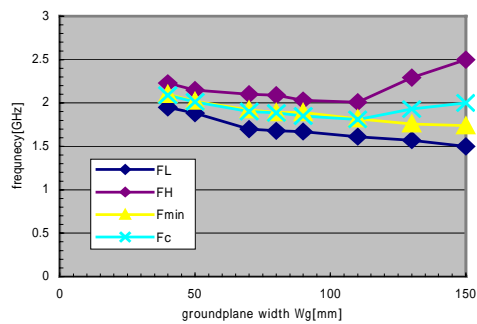
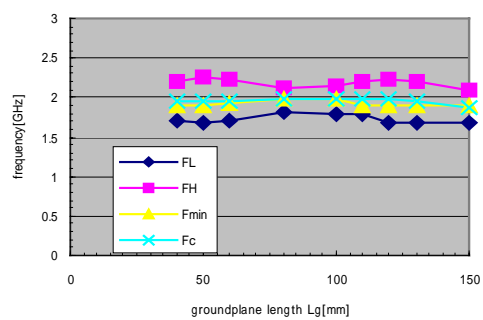


Fig. 4. Configuration of HIFA on a groundplane edge



(a) Dependence on groundplane width ($L_g=150$)



(b) Dependence on groundplane length ($W_g=80$)

Fig. 5. Resonance frequency characteristics as a function of groundplane size

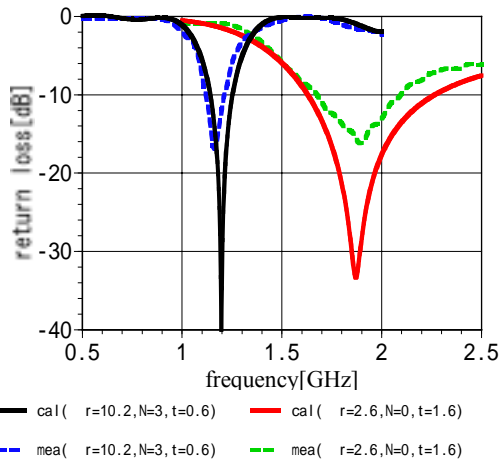


Fig. 6. Input characteristics of HIFA

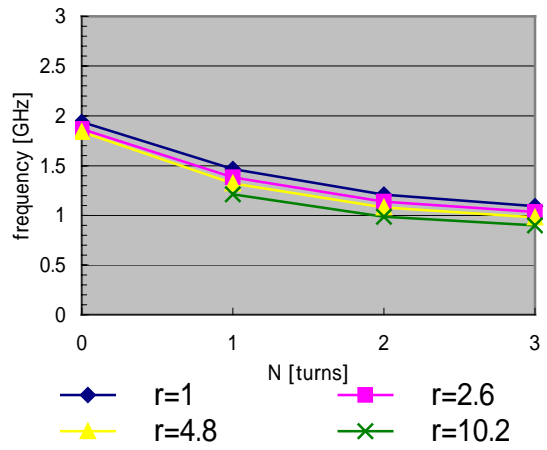


Fig. 7. Resonance frequency as a function of helix turn N and chip permittivity ϵ_r .

Table 1 Effective permittivity of dielectric material inside the helices

$\epsilon_r \backslash N$	0	1	2	3
2.6	1.08	1.13	1.13	1.06
4.8	1.11	1.24	1.25	1.12
10.2	-----	1.47	1.5	1.47

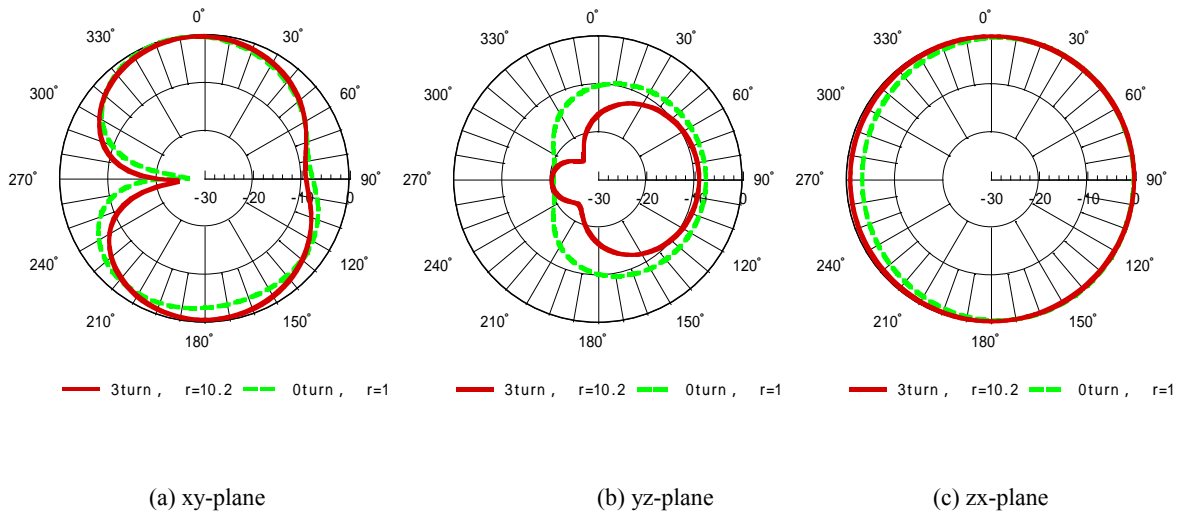


Fig. 8 Radiation Pattern ($t=1.6$ [mm])